EXPLORING THE STRUCTURAL MECHANICS OF TITANIUM NICKEL SOLID ALLOY USING COMSOL MULTIPHYSICS: A POISSON EQUATION AND CONTINUITY EQUATION PERSPECTIVE

*[1]P.J. Manga, [2]Mohammed Maina, [3]Samaila H., [4]E.W. Likta, [5]R.O. Amusat, [6]S. Daniel

[1* 3,4&5]Department of Physics, University of Maiduguri, Borno State, Nigeria
[2]Department of Chemical Engineering, Ramat Polytechnic Maiduguri, Borno State, Nigeria
[6]Department of Science Laboratory Technology, Abubakar Tatari Ali Polytechnic, Bauchi State, Nigeria

*Corresponding Author Email Address: 2016peterjohn@unimaid.edu.ng

ABSTRACT

This study investigates the structural mechanics of titanium-nickel (Ti-Ni) alloy thin film using computational modelling through COMSOL Multiphysics based on Poisson's equation and continuity equation for stress check by considering its linear elastic, conservation of charge and providing insight into nanomaterial deformation. In the COMSOL environment the parameters for titanium nickel (Ti-Ni) are embedded in the COMSOL Simulink interface. The Thin film layer was designed by defining the layer geometry of the size and shape of the layer with a width of $500 \ \mu m$, depth of $200 \ \mu m$ and height of $3 \ \mu m$ subjected to boundary conditions such as von – mises stress, surface temperature, iso-surface temperature, multi-slice electric potential, displacement component, surface elastic strain energy density and total enthalpy. The results displayed a trend that is, as the surface temperature increases there will be an increase in the current densities associated with high electrical conduction. On the same note, the designed thin film layer will pass the percolation threshold. The results of surface elastic strain energy density and total enthalpy imply that the designed thin film layer is effective and efficient as a structural pseudopotential device (photodiode).

INTRODUCTION

Thin film structural analysis of titanium nickel (Ti-Ni) is a crucial area of study in materials science and engineering. Titanium nickel, also known as nitinol, is a shape memory alloy with unique properties that make it valuable for various applications, including medical devices, actuators, sensors, and more (Binetti et al., 2019). Thin films of (Ti-Ni) offer additional advantages in terms of flexibility, reduced weight, and enhanced surface properties. In this article, we delve into the use of COMSOL Multiphysics software to analyse (Ti-Ni) alloys, focusing on the application of the Poisson equation and continuity equation (Romeo et al., 2021).

COMSOL Multiphysics offers a comprehensive platform for simulating the behaviour of complex materials like (Ti-Ni) alloys (Wang et al., 2018). The Poisson equation, which relates the material's deformation to its mechanical properties, and the continuity equation, ensuring mass conservation, play crucial roles in understanding the structural mechanics of (Ti-Ni) alloys (Ramanujam et al., 2020).

The Poisson equation describes the relationship between the lateral strain, longitudinal strain, and the material's elastic modulus (Caballero et al., 2014). By implementing this equation in COMSOL Multiphysics, engineers can visualize and analyse how (Ti-Ni) alloys deform under various loads and temperatures. This aids in optimizing the design of components subjected to mechanical stress, ensuring the material's longevity and reliability (Alamri et al., 2021).

The continuity equation, a fundamental principle in fluid dynamics and mass transport, is applied to (Ti-Ni) alloys to ensure mass conservation during phase transformations (Voznyia et al., 2020). As (Ti-Ni) undergoes martensitic phase transitions, mass redistribution occurs. COMSOL Multiphysics facilitates the modelling and analysis of these transformations, allowing engineers to predict material behaviour under different thermomechanical conditions (Banotra et al., 2020).

Titanium nickel exhibits a specific crystal structure at different temperatures. The thin film's crystal structure can influence its mechanical, thermal, and shape memory properties. Common crystal structures of (Ti-Ni) include austenite and martensite phases (Ahmmed et al., 2020).
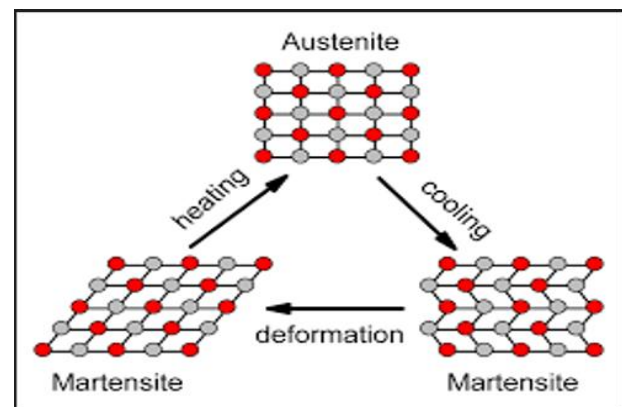

Figure 1: The plate of Titanium Nickel crystal structure (Gonzalez Flores et al., 2019)

The microstructure of a thin film refers to its small-scale features, such as grain size, orientation, and defects. Microstructural analysis provides insights into the film's mechanical strength, durability, and other mechanical properties (Zhao et al., 2021).
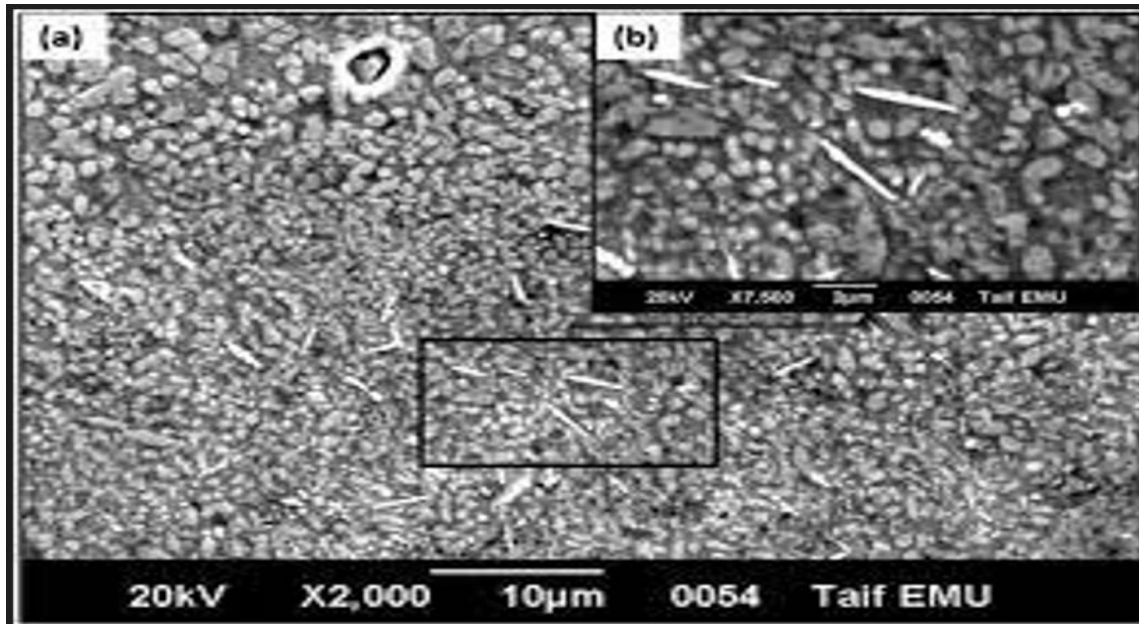
Exploring the Structural Mechanics of Titanium Nickel Solid Alloy Using Comsol Multiphysics: A Poisson Equation and Continuity Equation Perspective

71

Figure 2: The Plate of Titanium Nickel (Ti-Ni) - Solid Microstructure (Saxena et al., 2020)

In this work, we designed and simulated a Titanium Nickel (Ti-Ni) - Alloy thin film solar plate blind UV photodetector in 3D geometry using COMSOL Multiphysics software and analysed its structural mechanics and its response if been displaced (Zandi et al., 2020).

EXPERIMENT
Titanium nickel-based p-i-n structure thin film photodetector device is designed and simulated in 3D geometry using COMSOL Multiphysics software (Minbashi et al., 2018). The device is modelled with a defined material property embedded in COMSOL Multiphysics software. in the case of semiconductors, a module will be added and designed based on Poisson's Continuity equation. The p-i-n structure is effective as a photodiode device due to the high-sloped nature of its conduction and valence bands, which have the highest energy at varying conditions (Minbashi et al., 2018).

Simulation Parameters
On this note, we defined the simulated parameters required for the computational analysis based on titanium nickel-alloy using Comsol Multiphysics Simulink interface to assess the effect of the simulated thin film structural mechanics (Diachenko et al., 2019; Trenhame et al., 2011; Stelling et al., 2017: Garain et al., 2021; Manga et al., 2022; Ojinkwi et al., 2016; Minbashi et al., 2018).

Table 1: Simulation Defined Parameters

Name	Value	Unit
Density	$(\rho T(1/K))$ (Kg/m^3)	Kg/m^3
Thermal Conductivity	18	$W/(M.K)$
Heat capacity at constant pressure	837.36	$J/(Kg.K)$
Electrical conductivity	1219.5	S/m

Relative permittivity	1	1
Coefficient of thermal expansion	$11e^{-6}$	$1/K$
Young modulus	$E(T(1/K))\ (P_a)$	(P_a)
Poisson's ratio	0.33	1

Geometry Statistics
Geometric statistics is the most essential parameter needed for the effective design of the thin film layer which gives the space dimension, number of domains, number of boundaries, number of edges and number of vertices (Ullah et al., 2014; Diachenko et al., 2019; Trenhame et al., 2011; Stelling et al., 2017: Garain et al., 2021; Drummond et al., 1999; Ojinkwi et al., 2016; Minbashi et al., 2018; Cho et al., 2019).

Table 2: Geometry Statistics

Description	Value
Space dimension	3
Number of domains	1
Number of boundaries	6
Number of edges	12
Number of vertices	8

Thin Film Size and Shape
The size and shape help in defining the simulated thin film whether it is small or large. This gives a good definition of how portable the designed thin film layer is in terms of its width, Depth and Height vertices (Ullah et al., 2014; Diachenko et al., 2019; Trenhame et al., 2011; Stelling et al., 2017: Garain et al., 2021; Drummond et al., 1999; Ojinkwi et al., 2016; Minbashi et al., 2018; Cho et al., 2019).

Exploring the Structural Mechanics of Titanium Nickel Solid Alloy Using Comsol Multiphysics: A Poisson Equation and Continuity Equation Perspective

72

Table 3: Thin Film Design Parameter

Description	Value
Width	500
Depth	250
Height	3

MATERIALS AND METHODS

The semiconductor module in COMSOL uses the Poisson and continuity equations to simulate a semiconductor device. The Poisson equation is given as equations (1&2) (Xu et al., 2013).

$$\nabla(-\varepsilon_0 \varepsilon_r V) = q(p - n + Nd^+ - Na^-) \qquad (1)$$

where q is the electron charge, p and n are the hole and electron concentrations, respectively, and the charged impurities of donors and acceptors are denoted as Nd^+ and Na^- (Xu et al., 2013).

$$\frac{d^2}{dx^2}Q(x) = -\frac{dE(x)}{dx} = \frac{q}{\varepsilon}(n(x) - p(x) + N_a - N_d) \quad (2)$$

E is the electric field, Q is the particle charge, ε is the permittivity of the semiconductor, n and p are the free carrier's concentration whereby Nd^+, ε_r permittivity of reference material, ε_0 permitivity of a free space and Na are the concentration of acceptors and donors respectively (Dey et al., 2017).
The continuity equations are
For electrons, we have
$$\frac{\partial n}{\partial t} = \frac{1}{e}\overline{\nabla}.\overrightarrow{J_n} + G_n - R_n \qquad (3)$$

Similarly, for a hole, we have
$$\frac{\partial n}{\partial t} = -\frac{1}{e}\overline{\nabla}.\overrightarrow{J_n} + G_n - R_n \qquad (4)$$
The continuity equations can be derived from Maxwell's equations as given below:
$$\nabla J n = -qUn\nabla Jp = qUp \qquad (5)$$
Where,
G_n is the generation rate, R_n is recombination rate for the whole of the voulme of N-loop, j_n is the recombination current, qUp is the drift current which equal to the number of charge carriers. Q is the particle charge and ∇ laplacian operator.
Some **simulation** goal equations are given as follows
The simulation process was carried out under the following thin film computations for nitinol (NiTi-alloy) incorporated in Comsol Multiphysics Simulink tools in other to assess the index of nanomaterial linear elastic (Stress and Strain), heat conduction on the nanomaterial, thermal insulations, Current Conservation, Electric Insulation, terminals, Ground, Thermal expansion and Electromagnetic heating effect on the designed thin film layer (Lin et al., 2016).
The equation of the nanomaterial linear elasticity is given (Wangparawong et al., 2014)

$$0 = \nabla.S + F_v \qquad (6)$$
Where S is expressed as

$$S = S_{ad} + C/\epsilon_{el} \qquad (7)$$
$$\epsilon_{el} = \epsilon - C_{inel} \qquad (8)$$

$$C_{inel} = \epsilon_o + \epsilon_{ext} + \epsilon_{th} + \epsilon_{h5} + \epsilon_{pl} + \epsilon_{cr} \qquad (9)$$

$$S_{ad} = S_o + S_{ext} + S_q \qquad (10)$$

$$\epsilon = \frac{1}{2}(\{\nabla.u\}^T + \nabla.u) \qquad (11)$$

S total surface of the cell, u total energy, ϵ_{el} energy of the electron, ϵ_o permittivity of a free space, ϵ_{ext} external surface energy, ϵ_{th} thermal energy, ϵ_{pl} is the energy on the plate surface and ϵ_{h5} is the heat energy.
The equation for the heat conduction of titanium nickel NiTi-alloy is given (Ojinkwi et al., 2016)

$$eC_e u.\nabla T + \nabla.q = Q + Q_{ted} \qquad (12)$$

$$q = -K\nabla T \qquad (13)$$

The simulated thermal Insulation is defined by the given equation (Garain et al., 2021).

$$-nq = 0 \qquad (14)$$
The simulated temperature is taken as (Garain et al., 2021).

$$T = T_0 = 300K \qquad (15)$$
The simulated electrical current is given as (Stelling et al., 2017)

$$\nabla.J = Q_{j,v} \qquad (16)$$
$$J = \sigma E + Je \qquad (17)$$
$$E = -\nabla.V \qquad (18)$$
The simulated electric insulation is expressed as (Ahmmed et al., 2020)
$$n.J = 0 \qquad (19)$$
The ground and terminal are defined as (Diachenko et al., 2019)
$$V = 0 \qquad (20)$$
$$\int_{\partial\Omega}^0 J.nds = I_o \qquad (21)$$
The thermal expansion is defined as (Zhao et al., 2020)
$$\epsilon_{th} = \alpha(T)(T - T_{ref}) \qquad (22)$$
Electromagnetic heating is expressed as (Lin et al., 2016)
$$eC_p u.\nabla T = \nabla.(K\nabla T) + Q_e \qquad (23)$$
$$Q_e = J.E \qquad (24)$$
Q_e electron charge, K boltzman constant, C_p heat capacity, T absolute temperature, e strain energy density of the shell, u total energy, thermal expansion coefficient, T_{ref} references temperature, J current density, V surface volume, E electric field strength and ∇ laplacian operator.

RESULTS AND DISCUSSION
The meshing of the designed thin film layer was conducted under the following meshing statistics such as minimum element quantity, average element quantity, tetrahedron, triangle, edges element and vertex element (Ullah et al., 2014; Diachenko et al., 2019; Trenhame et al., 2011; Stelling et al., 2017: Garain et al., 2021; Drummond et al., 1999; Ojinkwi et al., 2016; Minbashi et al., 2018; Cho et al., 2019).

Table 4: Meshing Statistic

Description	Value
Minimum element quantity	0.002968
Average element quantity	0.2124
Tetrahedron	1909
Triangle	1384

Exploring the Structural Mechanics of Titanium Nickel Solid Alloy Using Comsol Multiphysics: A Poisson Equation and Continuity Equation Perspective

73

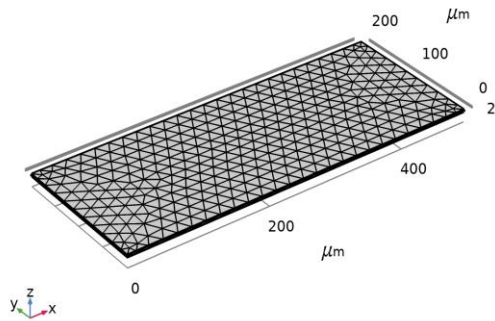|	
Edges element	152
Vertex element	8

Plate1: The meshing of the designed thin film

Simulated Results

The simulation results of structural mechanics were used to assess how effective and efficient the designed titanium nickel–alloy thin film layer is through contour flow under the following surface von-mises stress, surface temperature, isothermal contour, multi-slice electric potential, surface total displacement and surface electric strain energy density.

The results from **plate 2** show that the von-mises stress acting on the thin film surface displays low stress at a wavelength within the range of $0.25 \ \mu m - 0.45 \ \mu m$ while the surface temperature is recorded to be high at a value ranging from $0.5 \ \mu m - 2.0 \ \mu m$ of the nanomaterial. Due to a higher temperature, the carrier's concentration (while there are holes and electrons) depends exponentially on the energy band gap, Boltzmann's constant and absolute temperature. As the temperature decreases the corresponding rate of thermal generation of the intrinsic carriers decreases, as a result of that, the semiconductor will slowly behave like an insulator.
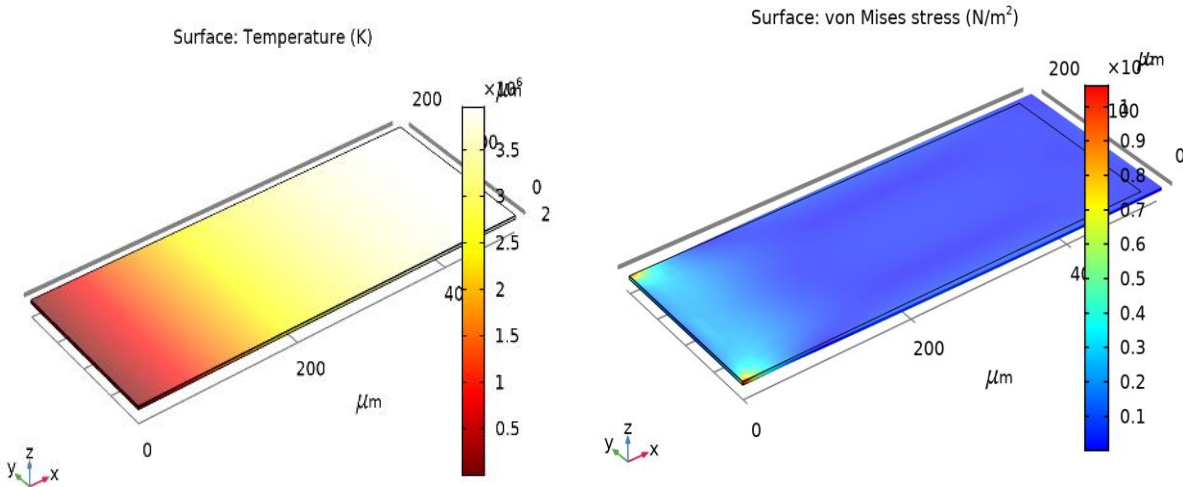

Plate 2: Surface von-mises (N/m^2) and temperature (K)

Plate 3 is the result of charge density based on charge conservation law which indicates that the simulated thin film displayed a good trend between iso-surface temperature and multi-slice electric potential. As the iso-surface temperature increases the electric potential also increases as shown, (and vice versa). This result is similar to work of (Ullah et al., 2014; Diachenko et al., 2019; Trenhame et al., 2011). In this case, the electric potential

spatial distribution in the designed thin film in terms of the magnitude of the iso-surface temperature it leads to higher current densities on the randomly oriented titanium nickel TiNi - alloy. It appears that the magnitude of current density is higher at extreme iso-surface temperature. The carrier's conduction is lower at lower iso-surface temperature but at extreme iso-surface temperature, the conductivity will be higher.
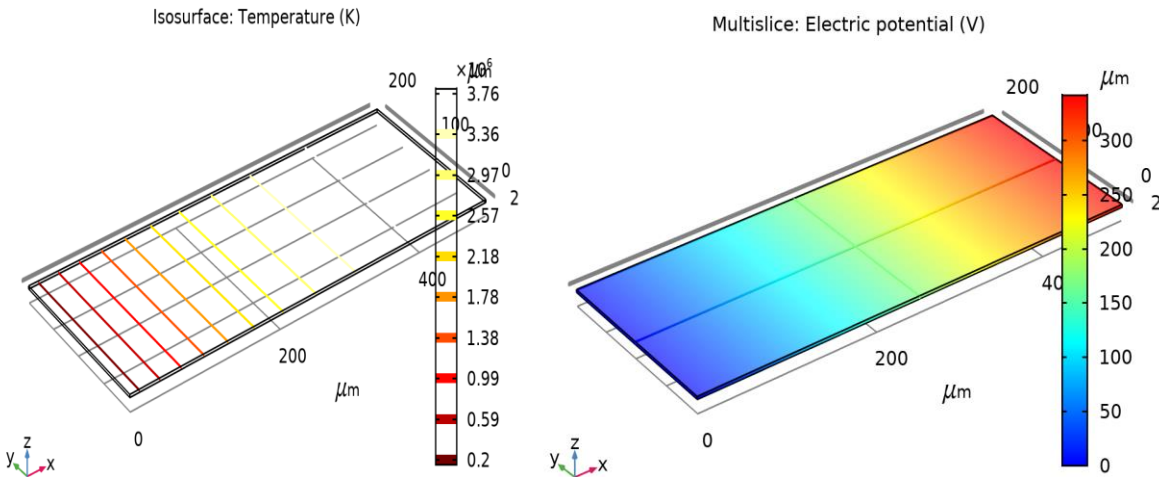
Exploring the Structural Mechanics of Titanium Nickel Solid Alloy Using
Comsol Multiphysics: A Poisson Equation and Continuity Equation Perspective

74

Plate 3: Iso-surface (K) and Multislice electric potential (V)

The results of the component displacement and total displacement of the designed thin film shown in **plate 4** imply that for a charged particle the ionizing energy loss predominates and leads to the production of electron–hole pairs. The simulated titanium nickel–alloy thin film was subjected to displacement component analysis to investigate the theory that a massive particle transfers momentum on the atoms in the solid, thereby displacing the atoms from their mean positions in the crystal lattice. The resulting unoccupying lattice site is called vacancy from our studies it was recorded within the range of $0 \, \mu m - 0.8 \, \mu m$ based on vertical displacement. At a displacement of $1 \, \mu m - 2 \, \mu m$, the displaced atoms eventually settle in a non-lattice position, known as

interstitial.

The Z-component implies that the incoming particle is high enough to displace several atoms and the displaced atoms themselves can displace other atoms on their way through the crystal creating a cluster of defects, which result in the change of optical and electrical properties of the designed thin film layer. This result is similar to that of Trenhame et al., (2011), were they conducted their research on two-dimensional linear elastic theory magneto-eletro-elastic plate to investigate the effect of piezoelectric, piezomagnetic and elastic cases. Their results show that surface effected by the thickness of the magneto-electro-elastic.
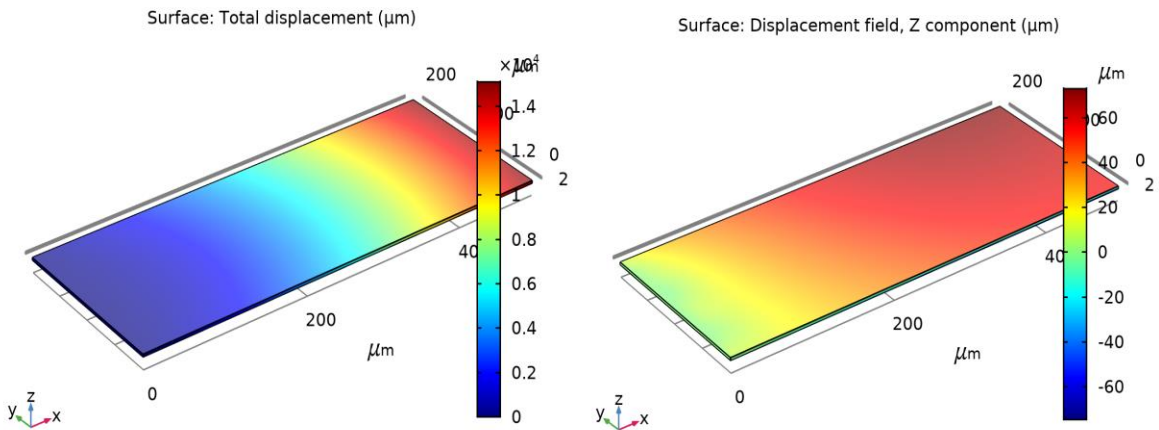

Plate 4: Total displacement (μm) and displacement field, X component (μm)

From **plate 5** are the results of elastic strain energy density and total enthalpy. The structural pseudopotential is extended to examine the effect of deformation of the strain energy density on the designed thin film. The results also show that the deformation of the thin film does not exhibit a particular trend with thermal

enthalpy. The plate shows that almost zero strain acts on the thin film therefore it is said to be more efficient and effective as a photodiode. Stelling et al., 2017 conducted a similar research where in their work they find out that the enthalpy is effected and induced by the strain energy density.
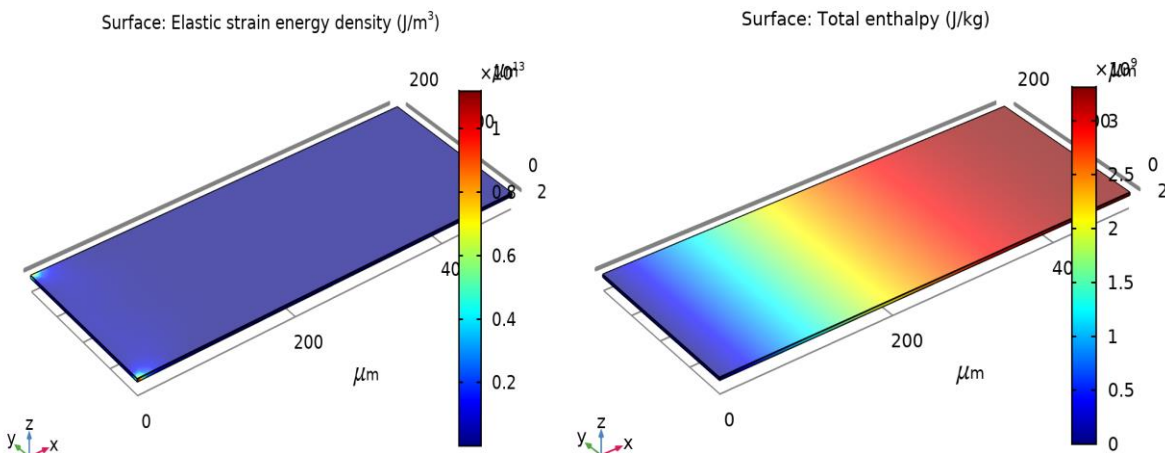
Exploring the Structural Mechanics of Titanium Nickel Solid Alloy Using
Comsol Multiphysics: A Poisson Equation and Continuity Equation Perspective

Plate 5: Surface elastic strain energy density (J/m^3) and total enthalpy (J/Kg)

Conclusion
COMSOL Multiphysics can solve a couple of physics problems by providing a powerful tool for exploring the structural mechanics of (Ni–Ti) alloys based on Poisson's equation and continuity equation. The simulation results of structural mechanics were used to assess how effective and efficient the designed titanium nickel–alloy thin film layer is through contour flow under the following surface von-mises stress, surface temperature, isothermal contour, multi-slice electric potential, surface total displacement and surface electric strain energy density. This shows that there is almost zero deformation coupled with high efficiency in the designed thin film layer. The results of this research can be used by scientists and engineers for future purposes (perovskite).

REFERENCES
A. Banotra, N. Padha, Facile growth of SnS and SnS0.40Se0.60thin films as an absorber layer in the solar cell structure, Mater. Today: Proc. 26 (2020) 3420– 3425, https://doi.org/10.1016/j.matpr.2019.11.154.

A. Romeo, E. Artegiani, CdTe-based thin film solar cells: past, present and future, Energies 14 (2021) 1684, https://doi.org/10.3390/en14061684.

A. Voznyia, V. Kosyak, Y. Yeromenko, J. Keller, A. Be¯rzina, A. Shamardin, I. Iatsunskyi, I. Shpetnyi, S. Plotnikov, A. Opanasyuk, Close-spaced sublimation of SnS absorber layers and SnS/CdS heterojunction solar cells with Mo and Ti back metal contacts, Thin Solid Films 709 (2020), https://doi.org/10.1016/j.tsf.2020.138153 138153.

A. Wangperawong, P.C. Hsu, Y. Yee, S.M. Herron, B.M. Clemens, Y. Cui, S.F. Bent, Bifacial solar cell with SnS absorber by vapour transport deposition, Appl. Phys. Lett. 105, 2014, 173904. 10.1063/1.4898092.

C. Stelling, C.R. Singh, M. Karg, T.A.F. König, M. Thelakkat, M. Retsch, Plasmonic nanomeshes: their ambivalent role as transparent electrodes in organic solar cells, Sci. Rep. 7 (2017) 42530.

H. Ullah, B. Marí, Numerical analysis of SnS based polycrystalline solar cells, Superlattices Microstruct. 72 (2014) 148–155, https://doi.org/10.1016/j.spmi.2014.03.042.

J. Ramanujam, M. Bishop, K. Todorov, O. Gunawan, R. Jatin Rath, E. Nekovei, A. R. Artegiani, Flexible CIGS, CdTe and a-Si: H based thin film solar cells: a review, Prog. Mater. Sci. 110 (2020), https://doi.org/10.1016/j. pmatsci.2019.100619 100619.

J. Xu, Y. Yang, Study on the performances of SnS heterojunctions by numerical analysis, Energy Convers. Manag. 78 (2014) 260–265, https://doi.org/10.1016/ j.enconman.2013.10.062.

J.Y. Cho, S. Sinha, M.G. Gang, J. Heo, Controlled thickness of a chemical-bath deposited CdS buffer layer for a SnS thin film solar cell with more than 3% efficiency, J. Alloys Compd. 796 (2019) 160–166, https://doi.org/10.1016/ j.jallcom.2019.05.035.

M. Dey, N. Maitry Dey, I. Rahman, R. Tasnim, U. Chakma, M.A. Aimon, N. Amin Matin, Numerical modelling of sns ultra-thin solar cells, in ECCE 2017 - International Conference on Electrical, Computer and Communication Engineering, 2017, pp. 911–915, https://doi.org/10.1109/ ECACE.2017.7913033.

M. Djinkwi Wanda, S. Ouédraogo, F. Tchoffo, F. Zougmoré, J.M.B. Ndjaka, Numerical investigations and analysis of Cu2ZnSnS4 based solar cells by SCAPS-1D, Int. J. Photoenergy 2016 (2016) 1–9, https://doi.org/10.1155/2016/ 2152018.

M. Minbashi, A. Ghobadi, M.H. Ehsani, H. Rezagholipour Dizaji, N. Memarian, Simulation of high efficiency SnS-based solar cells with SCAPS, Sol. Energy 176 176 (2018) 520–525, https://doi.org/10.1016/j.solener.2018.10.058.

O.V. Diachenko, O.A. Dobrozhan, A.S. Opanasyuk, D.I. Kurbatov, V.V. Grynenko, S.V. Plotnikov, Efficiency modelling of solar cells based on the n-Zn1-xMgxO / p-SnS Heterojunction, Journal of nano and electronic physics 11 (2019) 03024.

P. J. Manga[1], E.W. Likta[2], R.O. Amusat[3], S.D. Buteh[4], Muhammad Abubakar[5](2022); Optimization of Micro Horizontal

Exploring the Structural Mechanics of Titanium Nickel Solid Alloy Using Comsol Multiphysics: A Poisson Equation and Continuity Equation Perspective

76

Axis Wind Turbine Blade Using Computational Fluid Dynamic Analysis: International Journal of Modelling & Applied Science Research Published by Cambridge and Publications. Vol26 No.9, December, 2022.

P. Saxena, N.E. Gorji, COMSOL simulation of heat distribution in perovskite solar cells: coupled optical–electrical –thermal 3-D analysis, IEEE J. Photovolt. 9 (2019) 1693–1698, https://doi.org/10.1109/JPHOTOV.2019.2940886.

R. Caballero, E. Garcia-Llamas, J.M. Merino, M. Leon, I. Babichuk, V. Dzhagan, V. Strelchuk, M. Valakh, Non-stoichiometry effect and disorder in Cu2ZnSnS4 thin films obtained by flash evaporation: Raman scattering investigation, Acta Mater. 65 (2014) 412–417,
https://doi.org/10.1016/j.actamat.2013.11.010.

R. Garain, A. Basak, U.P. Singh, Study of thickness and temperature dependence on the performance of SnS-based solar cell by SCAPS-1D, Mater. Today: Proc. 39 (2021) 1833–1837, https://doi.org/10.1016/j.matpr.2020.06.185.

R.E. Treharne, A. Seymour-Pierce, K. Durose, K. Hutchings, S. Roncalli, D. Lane, Optical design and fabrication of fully sputtered CdTe/CdS solar cells, J. Phys: Conf. Ser. 286 (2011) 012038.

S. Ahmmed, A. Aktar, J. Hossain, A.B.M. Ismail, Enhancing the open circuit voltage of the SnS based heterojunction solar cell using NiO HTL, Sol. Energy 207 (2020) 693–702, https://doi.org/10.1016/j.solener.2020.07.003.

S. Alamri, M. Khushaim, S. Alamri, Preparation and characterization of Cu2ZnSnS4 thin films with various compositions deposited by a dual thermal evaporation technique, J. Alloys Compd. 870 (2021) 159392, https://doi.org/10.1016/j.jallcom.2021.159392.

S. Binetti, A. Le Donne, V. Trifiletti, New earth-abundant thin film solar cells based on chalcogenides, Front. Chem. 7 (2019) 297, https://doi.org/10.3389/fchem.2019.00297.

S. Lin, X. Li, H. Pan, H. Chen, X. Li, Y. Li, J. Zhou, Numerical analysis of SnS homojunction solar cell, Superlattices. Microstruct. 91 (2016) 375–382, https://doi.org/10.1016/j.spmi.2016.01.037.

S. Zandi, P. Saxena, N.E. Gorji, Numerical simulation of heat distribution in RGO-contacted perovskite solar cells using COMSOL, SolarEnergy 197 (2020) 105–110, https://doi.org/10.1016/j.solener.2019.12.050.

T. Drummond, Work Functions of the transition metals and metal silicides, 1999, 1–24. 10.1017/CBO9781107415324.004.

T.D. Lee, A.U. Ebong, A review of thin film solar cell technologies and challenges, Renew. Sust. Energ. Rev. 70 (2017) 1286–1297, https://doi.org/10.1016/j.rser.2016.12.028.

V.E. González-Flores, R.N. Mohan, R. Ballinas-Morales, M.T.S. Nair, P.K. Nair, Thin film solar cells of chemically deposited SnS of cubic and orthorhombic structures, Thin Solid Films 672 (2019) 62–65, https://doi.org/10.1016/j. tsf.2018.12.044.

X. Wang, R. Tang, C. Wu, C. Zhu, T. Chen, Development of antimony sulfide – selenide Sb2 (S, Se) 3-based solar cells, J. Energy Chem. 27 (3) (2018) 713–721, https://doi.org/10.1016/j.jechem.2017.09.031.

X. Zhao, L.M. Davis, X. Lou, S.B. Kim, S. Ulicna, A. Jayaraman, C. Yang, L.T. Schelhas, R. Gordon, Study of the crystal structure of SnS thin films by atomic layer deposition, AIP Adv. 11 (2021), https://doi.org/10.1063/5.0032782 035144.

Exploring the Structural Mechanics of Titanium Nickel Solid Alloy Using Comsol Multiphysics: A Poisson Equation and Continuity Equation Perspective

77